Journal of Alloys and Compounds 507 (2010) 376–379

Contents lists available at ScienceDirect

Journal of Alloys and Compounds

journal homepage: www.elsevier.com/locate/jallcom

Influence of hydrogen absorption on structural and magnetic properties of Ce_2Ni_2In

Wacław Iwasieczko, Dariusz Kaczorowski*

Institute of Low Temperature and Structure Research, Polish Academy of Sciences, Okolna 2, P.O. Box 1410, 50-950 Wrocław, Poland

ARTICLE INFO

Article history:
Received 24 June 2010
Received in revised form 26 July 2010
Accepted 28 July 2010
Available online 4 August 2010

Keywords:
Cerium intermetallics
Valence fluctuations
Hydrogenation

ABSTRACT

Hydrogenation studies were carried out on an intermediate-valence compound Ce_2Ni_2In. The alloy was found to absorb up to $x = 4.98$ hydrogen atoms per formula unit at 430 K and at a pressure of 0.3 MPa. The synthesized hydrides were stable in air for a period of few months. The hydrides with $x < 2$ retain the tetragonal Mo_2FeB_2-type structure (space group $P4/mbm$) of the parent compound. For larger hydrogen content a new hydride phase appears with an orthorhombic structure (space group $Pbam$). Along with the hydrogen uptake in $Ce_2Ni_2InH_x$ there occurs a change in the character of the electronic ground state related to the 4*f* electrons, from valence fluctuations in the parent compound to rather stable $4f^1$ configuration in the hydride with $x = 4.98$. Furthermore, for $x = 2.02$ and $x = 4.98$ long-range antiferromagnetic ordering is observed at low temperatures.

1. Introduction

Hydrogenation is known as an efficient method of tuning the electronic ground state properties in rare-earth intermetallics [1]. The most spectacular effect occurs in systems with unstable 4f shell, e.g. in Ce-based intermediate-valence compounds. In these materials, insertion of hydrogen atoms influences the hybridization between 4*f* electrons and conduction electrons via both an expansion of the unit cell and a change in the density of states at the Fermi level. As a result, the effective valence of cerium ions may vary as a function of the hydrogen content towards that corresponding to a stable $4f^1$ configuration in Ce^{3+}. The valence changes manifest themselves in the magnetic behavior of the hydrogenated system: features characteristic of valence fluctuations are gradually replaced by Curie–Weiss paramagnetism due to localized 4*f* electrons. Eventually, above a certain content of hydrogen atoms, a long-range magnetic ordering may occur at low temperatures. An excellent demonstration of such a behavior is the hydrogenation process of CeNiIn [1–3]. The parent compound is an intermediate-valence system with a Kondo temperature of 94 K, whereas the hydride $CeNiInH_{1.8}$ is a strong ferromagnet with the Curie temperature $T_C = 6.8$ K. Remarkably, hydrides of this alloy form with the same hexagonal ZrNiAl-type structure (space group $P\text{-}62m$) as CeNiIn, even though the hydrogenation causes a pronounced anisotropic expansion of the unit cell ($\Delta a/a = -3.1\%$ and $\Delta c/c = 16.4\%$ for the hydrogen content $x = 1.8$ [2]). In many other similar systems, insertion of hydrogen induces a change in the crystal structure. Such a symmetry transformation was observed for example in CeNiAl [4–7] that crystallizes in the ZrNiAl-type unit cell but its hydrides form with the AlB_2-type structure (space group $P6/mmm$). Apparently, the tetrahedral interstices in the parent structure are too small to accommodate the hydrogen atoms and the structural transition occurs. This symmetry transformation is accompanied by a rapid change of the electronic configuration of the cerium ions from intermediate-valence to nearly trivalent state. Similar behavior was also observed, e.g. for CeNiGa [8].

The ternary compounds Ce_2T_2In (T = 3*d*-, 4*d*-, 5*d*-electron transition metal) crystallize with the Mo_2FeB_2-type crystal structure (space group $P4/mbm$) [9]. Their physical properties were found to be mainly governed by the hybridization of 4*f* electrons with *d*-electrons of the ligands: whereas Ce_2Pd_2In, Ce_2Cu_2In and Ce_2Au_2In exhibit well-localized magnetism, Ce_2Ni_2In and Ce_2Rh_2In are intermediate-valence systems. The aim of the present work was to attempt affecting the electronic ground state in Ce_2Ni_2In by hydrogen atoms insertion. Recently, the results of a similar independent study were reported for the series $R_2Ni_2InH_x$ (R = La, Ce, Pr, Nd) where the hydrogen content was fixed to $x = 4.5$–5 [10]. It was found that upon hydrogen absorption the crystal structure changes into an orthorhombic one (space group $Pbam$), and this transition is accompanied with the unit cell volume increase by 10–20%. The latter paper, however, did not focus on the magnetic behavior of the hydrides of Ce_2Ni_2In, thus this data are communicated here for the first time.

* Corresponding author. Tel.: +48 71 34 350 21; fax: +48 71 34 410 19.
E-mail address: D.Kaczorowski@int.pan.wroc.pl (D. Kaczorowski).

0925-8388/$ – see front matter © 2010 Elsevier B.V. All rights reserved.
doi:10.1016/j.jallcom.2010.07.211

2. Experimental

Polycrystalline samples of Ce_2Ni_2In were synthesized by arc-melting stoichiometric amounts of the constituents (purity: cerium 99.8%, palladium 99.99%, indium 99.99%) under titanium-gettered argon atmosphere. The ingots were turned over and remelted several times to ensure homogeneity. Weight losses during the arc-melting were smaller than 0.5 wt%. Quality of the products was checked by X-ray powder diffraction using a Stoe powder diffractometer with Cu $K\alpha_1$ radiation.

Hydrogen absorption experiments were performed in a classical Sievert's-type apparatus adopted for PTC measurements. Powder samples were placed in reaction chamber and heated under vacuum (5×10^{-5} Pa) at a temperature of 473 K for 4 h. After activation process the samples were cooled down to room temperature in vacuum, and then exposed to hydrogen gas at a pressure of few atmospheres. The synthesis reaction took place at the temperature range 340–430 K. The hydride with the highest content of hydrogen ($x = 4.98$) was prepared at 430 K by the application of hydrogen pressure of 0.3 MPa. Subsequently, the hydrides were slowly cooled down to room temperature at a rate of 3 K per hour. The amount of hydrogen in the samples was determined with the accuracy of ±0.02 hydrogen atoms per formula unit (H/f.u.) by measuring the hydrogen pressure drop in a calibrated apparatus volume. All the hydrides were examined by X-ray powder diffraction (equipment as above) using silicon as an internal standard. The unit cell parameters were calculated using the program DICVOL [11]. All the synthesized hydrides were stable in air for a period of few months.

Magnetic measurements were performed in the temperature range 1.8–300 K and in applied magnetic fields up to 5 T employing a commercial superconducting quantum interference device (SQUID) magnetometer. For these measurements loose powders were utilized which were placed in small gelatin capsules.

3. Results and discussion

3.1. Crystal structures

The X-ray powder diffraction examinations confirmed that the parent compound Ce_2Ni_2In crystallizes with the Mo_2FeB_2-type structure (space group $P4/mbm$). The refined tetragonal lattice parameters $a = 0.7521(2)$ nm and $c = 0.3717(1)$ nm are very close to those reported in the literature [9]. This crystal structure (in the following called α-phase) was found to be stable in the $Ce_2Ni_2InH_x$ hydrides up to the hydrogen content $x = 2$. For larger x one observes on the diffraction patterns the appearance of several other peaks besides those corresponding to the Mo_2FeB_2-type unit cell, which can be indexed assuming the orthorhombic symmetry $Pbam$ (subsequently called β-phase), reported in Ref. [10] for $Ce_2Ni_2InH_5$. The relative intensities of the Bragg peaks due to the α- and β-phases gradually change with increasing the hydrogen content, and for $x = 4.98$ a nearly single β-phase pattern is observed, as demonstrated in Fig. 1.The refined lattice parameters of the α-type $Ce_2Ni_2InH_x$ hydrides manifest a minor anisotropic expansion of the unit cell with increasing the hydrogen content. As is apparent from Table 1, the lattice parameter a decreases, while the parameter c increases with rising x. Remarkably, the unit cell volume of $Ce_2Ni_2InH_2$ is only about 0.5% larger than that of the parent compound. For further increase of x, the α-phase observed on the X-ray patterns does not exhibit any further change in the lattice parameters, and the β-phase keeps the values $a = 0.8976(3)$ nm, $b = 0.7537(2)$ nm, $c = 0.3720(1)$ nm, which correspond also to the hydride $Ce_2Ni_2InH_{4.98}$. Clearly, the compositions $2 < x < 4.98$ define a mixed two-phases region. The unit cell volume of $Ce_2Ni_2InH_{4.98}$ is about 19% larger than that of Ce_2Ni_2In. It is worth noting that heating the orthorhombic hydride $Ce_2Ni_2InH_{4.98}$ up to 1070 K results in its complete decomposition, and the α-type tetragonal structure of Ce_2Ni_2In is fully recovered.

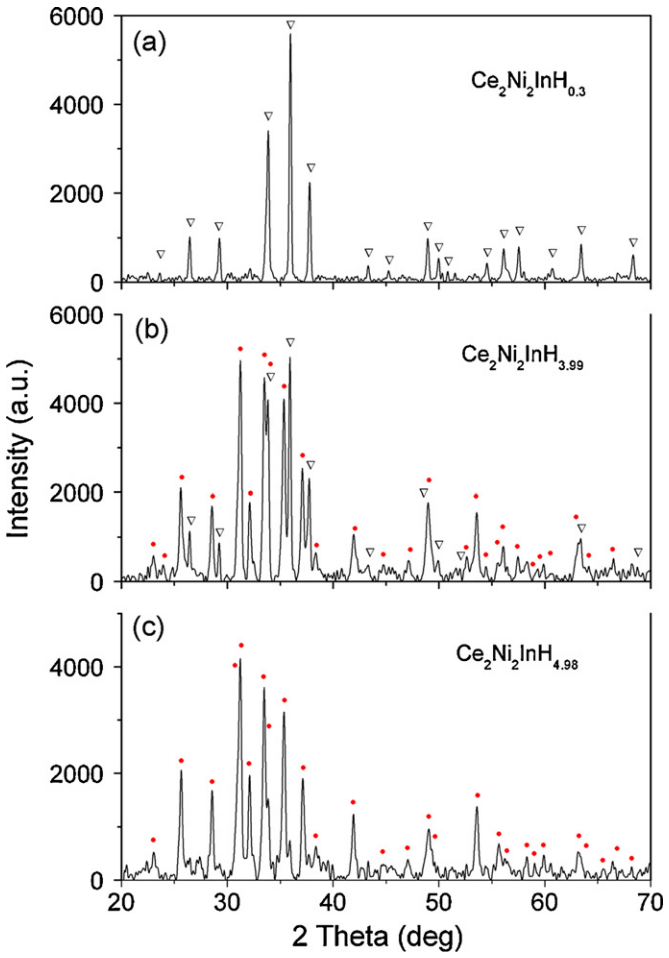

Fig. 1. X-ray powder diffraction patterns of $Ce_2Ni_2InH_x$ for $x = 0.3$ (a), $x = 3.99$ (b), and $x = 4.98$ (c). The Bragg peaks marked by triangles correspond to the tetragonal α-phase, while those marked by dots originate from the orthorhombic β-phase.

3.2. Magnetic properties

3.2.1. $Ce_2Ni_2InH_x$ hydrides with $x \leq 2.02$

The temperature dependencies of the inverse molar magnetic susceptibility of the α-type $Ce_2Ni_2InH_x$ hydrides are presented in Fig. 2. The data obtained for the parent compound Ce_2Ni_2In is very similar to those reported in Ref. [9]. Its magnetic susceptibility is very small (of the order of 10^{-4} emu/mole$_{Ce\text{-}atom}$) and only weakly temperature dependent. In the high temperature region, $\chi^{-1}(T)$ exhibits a broad shallow minimum centered around $T_{min} = 380$ K.

Table 1
Crystallographic data of $Ce_2Ni_2InH_x$ ($x = 0$–4.98).

Compound	Space group	a (nm)	b (nm)	c (nm)	c/a	V (nm^3)
Ce_2Ni_2In	$P4/mbm$	0.7521(2)	–	0.3717(1)	0.494	0.2103
$Ce_2Ni_2InH_{0.05}$	$P4/mbm$	0.7521(2)	–	0.3717(2)	0.494	0.2103
$Ce_2Ni_2InH_{0.15}$	$P4/mbm$	0.7512(4)	–	0.3718(3)	0.495	0.2098
$Ce_2Ni_2InH_{0.30}$	$P4/mbm$	0.7520(2)	–	0.3719(2)	0.495	0.2103
$Ce_2Ni_2InH_{1.00}$	$P4/mbm$	0.7524(2)	–	0.3720(2)	0.494	0.2106
$Ce_2Ni_2InH_{1.57}$	$P4/mbm$	0.7526(4)	–	0.3719(3)	0.494	0.2106
$Ce_2Ni_2InH_{1.82}$	$P4/mbm$	0.7530(2)	–	0.3721(1)	0.494	0.2110
$Ce_2Ni_2InH_{2.00}$	$P4/mbm$	0.7531(2)	–	0.3728(2)	0.495	0.2113
$Ce_2Ni_2InH_{4.98}$	$Pbam$	0.8976(3)	0.7537(2)	0.3720(1)	0.414	0.2517

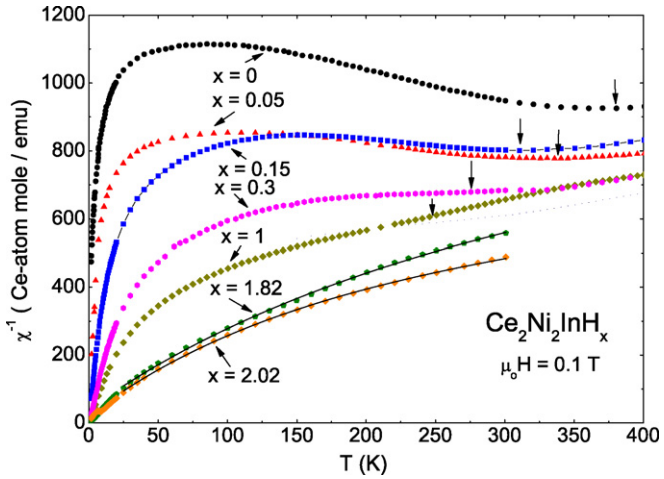

Fig. 2. Temperature dependencies of the inverse molar magnetic susceptibility of $Ce_2Ni_2InH_x$ with the hydrogen content $x = 0$–2.02, measured in a magnetic field of 0.1 T. The arrows mark the temperatures T_{min} (see the text). The solid lines for $Ce_2Ni_2InH_{1.82}$ and $Ce_2Ni_2InH_{2.02}$ represent the MCW fits discussed in the text.

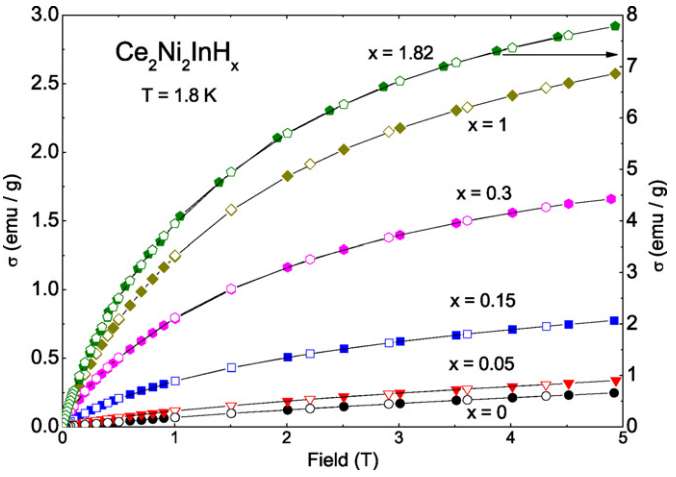

Fig. 3. Field dependencies of the magnetization of $Ce_2Pd_2InH_x$ with the hydrogen content $x = 0$–1.82, taken at 1.8 K with increasing (full symbols) and decreasing (open symbols) magnetic field. Note a different vertical scale for $Ce_2Ni_2InH_{1.82}$.

This behavior characterizes valence fluctuations with the characteristic energy scale $T_{sf} = 3T_{min}/2 = 570$ K [12]. Somewhat more distinct temperature variation of the magnetic susceptibility is observed at low temperatures, which may be ascribed to the presence of small amounts of stable Ce^{3+} ions, likely located at grain boundaries or on surfaces of powder particles. With increasing the hydrogen content the magnitude of the magnetic susceptibility increases, and the minimum gradually shifts towards lower temperatures. For the hydrides with $x = 0.05$, 0.15, 0.3 and 1, T_{min} is about 337, 310, 275 and 247 K, respectively. This behavior manifests a systematic decrease of the spin-fluctuation temperature T_{sf} that for Ce_2Ni_2InH amounts to about 370 K. In parallel to those changes, the low-temperature downturn in the inverse magnetic susceptibility gradually increases with raising the hydrogen content. All these features indicate that along the series the effective valence of Ce ions changes towards +3.

For the hydrides with $x > 1$ no local minimum in $\chi^{-1}(T)$ can be discerned. Nevertheless, the overall behavior of the magnetic susceptibility indicates that also for these compounds significant valence instabilities occur. As apparent from Fig. 2, the magnetic susceptibility of the compounds having the compositions close to $x = 2$, can be described over a large temperature range (above 50 K) by a modified Curie–Weiss law $\chi = \chi_0 + C/(T - \theta_p)$, which points to a tendency towards stabilization of the 4*f* state. Remarkably, the paramagnetic Curie temperature θ_p derived for $Ce_2Ni_2InH_{1.82}$ and $Ce_2Ni_2InH_{2.02}$ is rather small being equal to −11.9(4) and −4.2(2) K, respectively. Such magnitude of θ_p is a typical feature of cerium intermetallics with localized 4*f* electrons. On the other hand, the effective magnetic moment $\mu_{eff} = (8C)^{1/2}$ derived per Ce-ion for $Ce_2Ni_2InH_{1.82}$ amounts to only 1.55(2) μ_B and that found for $Ce_2Ni_2InH_{2.02}$ is $\mu_{eff} = 1.57(2)\,\mu_B$. It is to be noted that these values of μ_{eff} are much smaller than that expected within the Russell–Saunders coupling scheme for stable trivalent cerium ion (2.54 μ_B), which implies still rather large degree of 4*f* electron delocalization. Another hint at fairly unstable 4*f* shell in these two hydrides comes from the rather enhanced magnitude of the temperature-independent contribution χ_0 equal to $0.78(5) \times 10^{-3}$ and $1.12(4) \times 10^{-3}$ emu/mole$_{Ce\text{-}atom}$ for $Ce_2Ni_2InH_{1.82}$ and $Ce_2Ni_2InH_{2.02}$, respectively.

The increasing degree of localization of the cerium 4*f* electron with the rise in the hydrogen content in the $Ce_2Ni_2InH_x$ hydrides may be also figured out from the field variations of the magnetization. As shown in Fig. 3, on going from $x = 0$ to $x = 1$ the magnetization gradually increases and the $\sigma(H)$ function becomes more and more curvilinear. The changes are even more prominent on proceeding to $x = 1.82$ (note a different vertical scale in Fig. 3). This behavior straightforwardly manifests systematic enhancement in the magnitude of the cerium magnetic moment along the series.

The low-temperature magnetic behavior in $Ce_2Ni_2InH_{2.02}$ is zoomed-in in Fig. 4. As may be inferred from the observed maximum in $\chi(T)$ the compound orders antiferromagnetically at $T_N = 8.5(2)$ K. In the ordered region, the magnetic susceptibility shows a pronounced upturn that may indicate that not all cerium atoms are involved in the magnetic ordering. Alternatively, complex antiferromagnetic structure might be anticipated. The antiferromagnetic ground state in $Ce_2Ni_2InH_{2.02}$ is further corroborated by the magnetization data studied as a function of the magnetic field strength. As displayed in the inset to Fig. 4, while the $\sigma(H)$ isotherm measured at 10 K is characteristic for paramagnetic region, those taken at 1.8 K and 5 K exhibit clear metamagnetic-like anomalies in a field slightly larger and smaller than 3 T, respectively. The transition observed at 1.8 K is very sharp and reveals distinct hysteresis in the field-induced ferromagnetic state. At 5 K, both fea-

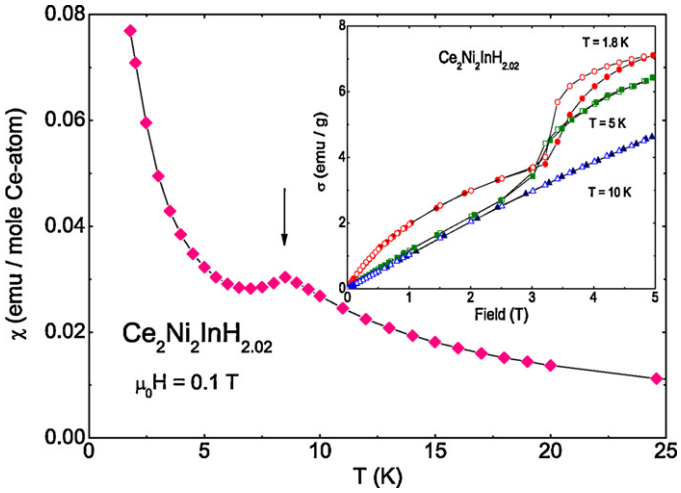

Fig. 4. Low-temperature variation of the molar magnetic susceptibility of $Ce_2Ni_2InH_{2.02}$ measured in a magnetic field of 0.1 T. The arrow marks the antiferromagnetic phase transition. The inset displays the magnetization isotherms taken at 1.8, 5 and 10 K with increasing (full symbols) and decreasing (open symbols) magnetic field.

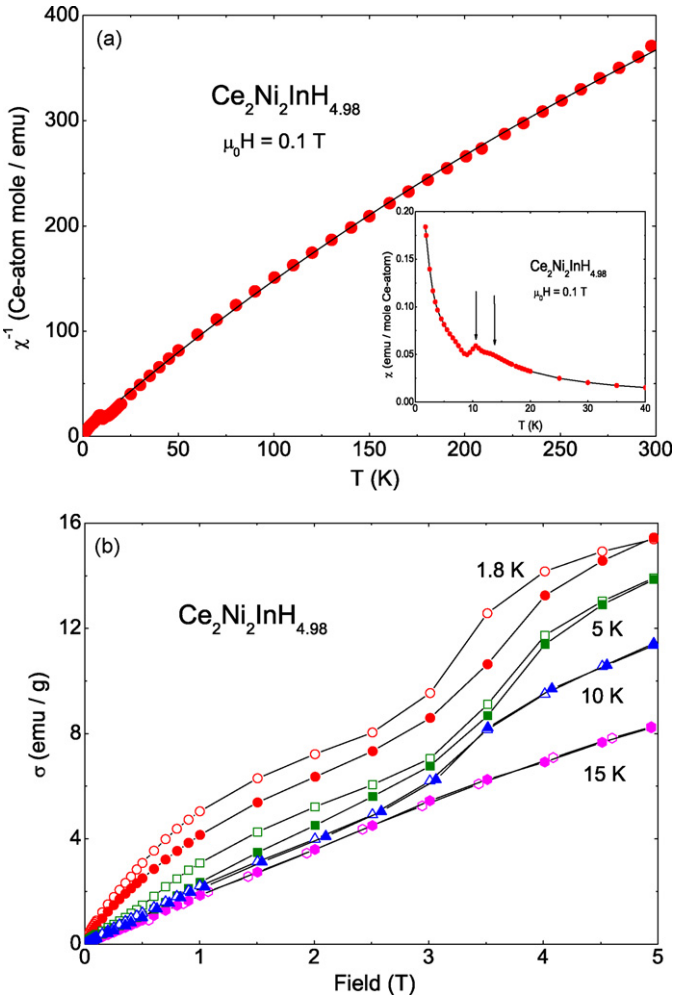

Fig. 5. (a) Temperature dependence of the inverse molar magnetic susceptibility of $Ce_2Ni_2InH_{4.98}$ measured in a magnetic field of 0.1 T. The solid line is the MCW fit discussed in the text. The inset shows the low-temperature variation of the molar magnetic susceptibility. The arrows indicate the magnetic phase transitions. (b) Field dependencies of the magnetization of $Ce_2Ni_2InH_{4.98}$ taken at 1.8, 5, 10 and 15 K with increasing (full symbols) and decreasing (open symbols) magnetic field.

tures are much less pronounced. Another noteworthy difference between the two magnetization isotherms is in their shapes below the critical field. Whereas $\sigma(H)$ measured at 5 K shows a straight-line behavior typical of simple antiferromagnets, the magnetization taken deeply in the ordered state is a strongly curvilinear function of the magnetic field. The latter effect seems in line with the afore-mentioned tail in $\chi(T)$ below about 5 K, and thus supports the hypothesis on the complex antiferromagnetic structure in this hydride.

3.2.2. $Ce_2Ni_2InH_{4.98}$

The magnetic properties of the terminal hydride $Ce_2Ni_2InH_{4.98}$ are summarized in Fig. 5. At low temperatures, the magnetic susceptibility shows a complex temperature variation with two local maxima at $T_{N1} = 13.2(4)$ K and $T_{N2} = 10.5(2)$ K, and a substantial upturn below 9 K (see the inset to Fig. 5a). Apparently, the magnetic behavior in this compound is fairly complex. This complexity is seen also in the magnetic field dependencies of the magnetization, presented in Fig. 5b. The magnetization isotherm measured at 1.8 K is somewhat akin to that observed at this temperature for $Ce_2Ni_2InH_{2.02}$, however the hysteresis effect is seen here in the entire magnetic field range, i.e. not only above a critical field of about 3 T in which a metamagnetic-like phase transition takes place. Similar sigmoid-shaped $\sigma(H)$ variations appear also at 5 and 10 K but the hysteresis distinctly diminishes and it is hardly seen just below T_{N2}. The magnetization studied at 15 K is proportional to the magnetic field strength, as can be expected for a paramagnet.

In the paramagnetic region (above about 30 K), the magnetic susceptibility of $Ce_2Ni_2InH_{4.98}$ follows the modified Curie–Weiss law with the effective magnetic moments $\mu_{eff} = 2.24(1)\,\mu_B$ per Ce atom, the paramagnetic Curie temperature $\theta_p = -2.8(2)$ K, and the constant term $\chi_0 = 0.65(2) \times 10^{-3}$ emu/mole$_{Ce\text{-}atom}$. It is worth noting that the experimental value of μ_{eff} is much closer to that calculated for a free trivalent cerium atom than in all the hydrides with smaller hydrogen content. This feature implies significant change in the valence state of the Ce ions in the $Ce_2Ni_2InH_x$ system in the upper limit of hydrogenation.

For all the hydrides with the hydrogen index $2.02 < x < 4.98$, the magnetic susceptibility curves revealed the presence of three anomalies at about 13.2, 10.5 and 8.5 K, which arise from simple superposition of the magnetic properties of $Ce_2Ni_2InH_{2.02}$ and $Ce_2Ni_2InH_{4.98}$. This finding is in line with the X-ray data that showed the hydrides from this region to be composed of the two terminal phases.

4. Conclusions

The intermetallic compound Ce_2Ni_2In easily absorbs hydrogen up to the composition $Ce_2Ni_2InH_{4.98}$, in good agreement with the previous report [10]. The tetragonal structure of the Mo_2FeB_2-type accommodates the hydrogen atoms up to $x \approx 2$ with insignificant expansion of the lattice. For larger hydrogen content two-phase region is observed in which the tetragonal phase $Ce_2Ni_2InH_2$ is accompanied by the orthorhombic phase $Ce_2Ni_2InH_{4.98}$. The relative amounts of these phases depend on the hydrogen index x.

Hydrogenation of Ce_2Ni_2In leads to a systematic change in the electronic ground state properties. With increasing the hydrogen content in $Ce_2Ni_2InH_x$ one observes first continuous development of the magnetic moments carried by the cerium ions. The macroscopic magnetic properties evolve from those characteristics of strongly intermediate-valence systems towards those typical for stable moment paramagnets. For $Ce_2Ni_2InH_{2.02}$, the terminal tetragonal hydride, as well as for the orthorhombic hydride $Ce_2Ni_2InH_{4.98}$ some complex antiferromagnetic behavior was revealed at low temperatures. More detailed description of the ordered ground states in these two phases requires further experimental efforts, preferably neutron diffraction studies on the corresponding deuterides.

References

[1] I.I. Byluk, V.A. Yartys, R.V. Denys, Ya.M. Kalychak, I.R. Harris, J. Alloys Compd. 284 (1999) 256.
[2] B. Chevalier, M.L. Kahn, J.-L. Bobet, M. Pasturel, J. Etourneau, J. Phys.: Condens. Matter 14 (2002) L365.
[3] K. Shashikala, A. Sathyamoorthy, P. Raj, S.K. Dhar, S.K. Malik, J. Alloys Compd. 437 (2007) 7.
[4] B. Bandyopadhyay, K. Ghoshray, A. Ghoshray, N. Chatterjee, Phys. Rev. B 38 (1988) 8455.
[5] J.-L. Bobet, B. Chevalier, B. Darriet, M. Nakhl, F. Weill, J. Etourneau, J. Alloys Compd. 317–318 (2001) 67.
[6] B. Chevalier, M. Pasturel, J.-L. Bobet, R. Decourt, J. Etourneau, O. Isnard, J. Sanchez Marcos, J. Rodriguez Fernandez, J. Alloys Compd. 383 (2004) 4.
[7] K. Shashikala, A. Sathyamoorthy, P. Raj, W.B. Yelon, S.K. Malik, J. Alloys Compd. 438 (2007) 84.
[8] B. Chevalier, J.-L. Bobet, E. Gaudin, M. Pasturel, J. Rtourneau, J. Solid State Chem. 168 (2002) 28.
[9] D. Kaczorowski, P. Rogl, K. Hiebl, Phys. Rev. B 54 (1996) 9891.
[10] M. Dzevenko, K. Miliyanchuk, Ya. Filinchuk, O. Stelmakhovych, L. Akselrud, L. Havela, Ya.M. Kalychak, J. Alloys Compd. 447 (2009) 182.
[11] A. Boultif, D. Louer, J. Appl. Cryst. 37 (2004) 724.
[12] J.M. Lawrence, P.S. Riseborough, R.D. Parks, Rep. Prog. Phys. 44 (1981) 1.